Supplementary Materials for

Asymmetric apportioning of aged mitochondria between daughter cells is required for stemness

Pekka Katajisto*, Julia Döhla, Christine Chaffer, Nalle Pentinmikko, Nemanja Marjanovic, Sharif Iqbal, Roberto Zoncu, Walter Chen, Robert A. Weinberg, David M. Sabatini*

*correspondence to: pekka.katajisto@helsinki.fi or sabatini@wi.mit.edu

This PDF file includes:

Other Supplementary Materials for this manuscript includes the following:

Supplementary movies S1 to S5

Materials and Methods

Constructs and lentiviral infections

The vectors for lentiviral expression of fusion proteins were generated by replacing the GFP of pLJM2 (*1*) with paGFP (*2*) or Snap-tag (New England Biolabs) by PCR-cloning with MluI-EcoRI digestion for C-terminal tags and NheI-MluI for N-terminal tags. The resulting vectors were then modified with PCR-cloning of the localization signals or full-length proteins with previously reported localization to targeted organelles.

Primers used:

PAGFP-N_NheI-Kozak_F	CTGACGCTAGCGCCACCATGGTGAGCAAGGGCGAGG
PAGFP-N_EcoR1-MluI_R	CTCTAGAATTCACGCGTCTTGTACAGCTCGTCCATGCC
PAGFP-C_NheI-MluI_F	CTGAGCTAGCACGCGTATGGTGAGCAAGGGCGAGG
PAGFP-C_EcoR1_STOP_R	TCTAGAATTCTTACTTGTACAGCTCGTCCATG
SNAP-TAG-N-NheI-Kozak-F	CTGACGCTAGCGCCATGGACAAAGATTGCGAAATGAAACGTACCA
SNAP-TAG-N-Mlu-R	CTCTAACGCGTGGATCCTGGCGCGCCTATACCTG
SNAP-TAG-C-Mlu-F	CTCTAACGCGTATGGACAAAGATTGCGAAATGAAACGTACCA
SNAP-TAG-C-EcorI-Stop-R	TCTAGAATTCTTAGGATCCTGGCGCGCCTATACCTG
Omp25_N-term_F	CTGACGCTAGCGCCATGGGGCGAGGCGACGGAGAGCCG
Omp25_N-term_R	CTCTAACGCGTGAGCTGCTTTCGGTATCTCAC
H2B-N-NheI-Kozak-F	CTGACGCTAGCGCCACCATGCCTGAACCGGCAAAATC
H2B-N-Mlu-R	CTCTAACGCGTCTTGGAGCTGGTGTACTTG
Rpl10a-C-Mlu-F	CTCTAACGCGTATGAGCAGCAAAGTCTCTCG
Rpl10a-C-EcorI-Stop-R	TCTAGAATTCTTAATATAGGCGCTGGGGC
Lamp2-N-NheI-Kozak-F	CTGACGCTAGCGCCATGGTGTGCTTCCGCCTCTTC
Lamp2-N-Mlu-R	CTCTAACGCGTCACAGACTGATAACCAG
COX8a-N-NheI-Kozak-F	CTGACGCTAGCGCCATGTCCGTCCTGACGCCGCTGCTG
COX8a-N-Mlu-R	CTCTAACGCGTGAGACCGGAGGACATCCAGAGGTC

Lentivirus were produced in 293T cells using standard methods. Briefly, 140,000 cells were seeded on a 6-well plate, cultured o/n, and co-transfected using FuGENE-6 reagent (Roche) with 900ng of packaging plasmid pCMV-dR8.91, 100ng of envelope plasmid VSV/G, and 1µg of the organelle targeting vector. Transfection media was removed 16 hours later and replaced with DMEM containing 10% IFS. Virus containing media was harvested 24h later.

Human mammary epithelial cell (hMEC) derived stem-like cells (SLCs) were cultured as previously described (*3*). Cells were maintained in MEGM Mammary Epithelial Cell Growth Medium (Lonza) or CnT-27 PCT Mammary Epithelium Medium (CELLnTECH Advanced Cell Systems). For live imaging, cells were maintained in phenol-red free media containing full supplements. Cells cultured in CnT-27 were used for autophagy assays, and live imaging of Snap-tag labeled cells loaded with MitoTracker Green FM (Life Technologies), or LysoTracker Green DND-26 (Life Technologies), respectively.

Cells were infected with 70µl of lentivirus containing media on 6-well plates in the precence of 8µg/ml of polybrene. Cells were selected with 2µg/ml puromycin for 3 days.

Two previously characterized cell lines (FL1, FL2) (*3*) were analyzed, and they functioned similarly in all the performed assays.

For Snap-tag expressing cells, the cells were further selected by labeling with Snap-Cell TMR-Star (see below) and by cell sorting to isolate cells with similar expression levels of mitochondrial Snap-tags.

Imaging and photoactivation

SLCs stably expressing paGFP-fusion proteins were imaged on a spinning disk confocal system (Andor and Nikon), with Andor IQ acquisition software and Andor iXion+ EMCCD cameras. During imaging, cells were maintained in LiveCell Stagetop incubation system (+37°C, 5% CO_2) on a glass bottom culture dish (MatTek P35GC-1.5-14-C), in phenol-red free cell culture media containing full supplements.

Photoactivation was conducted with Andor Revolution FRAPPA device, using the 405nm laser at 10% and 100ms bursts, at multiple locations within the cell. Organelles in approximately 20% of the cell's total area were photoactivated as uniform activation even in the cytoplasm was toxic to cells and inhibited division. The morphology of cells (round vs flat) was determined with DIC objective immediately after photoactivation, but before time-lapse imaging for apportioning during division. Photoactivated cells were imaged with 488nm excitation at 10-20% power, 20-60ms exposure time, and camera gain at maximum to reduce phototoxicity. Images were recorded every 1-3min to create the time-lapse movies, and to capture divisions. Focus plane was automatically maintained (Nikon Perfect focus system). 20X objective was used to allow for cell motility during imaging. Imaging of Snap-tag labeled mitochondria was conducted similarly to paGFP, with additional images of the red label captured with 20% laser power and 30ms exposure. 20X and 40X objectives were used to analyze division and label localization, respectively.

For high-resolution imaging at individual timepoints and analysis of fixed samples, cells were grown on glass bottom dishes (MatTek P35G-1.5-10-C) coated with fibronectin (Sigma-Aldrich) to a density of 100,000 cells per dish at the time of imaging or fixation. Imaging was conducted on a spinning disk confocal system (3i, Yokogawa, Semrock) using 63X objective and 1.6X optical zoom, with Slidebook 5.5 acquisition software (3i) and Andor Neo sCMOS camera. For live cell imaging, cells were maintained at +37°C, 5% CO_2 in "The Cube & The Box" incubation system (Life Imaging Services).

Snap-tag labeling, cell synchronization, and analysis of asymmetric division

For synchronization, cells were cultured in the presence of 2mM thymidine for 19 hours, followed by 3x washing with PBS and trypsination. After trypsin inactivation and

centrifugation, Snap-tag expressing cells were treated with Snap-Cell substrates (New England Biolabs) as indicated to label old mitochondria. Cells were washed three times with PBS or culture medium and plated in full MEGM. In case of synchronization, thymidine was added 10 hours later, and removed 27 hours later by 3x PBS washings. After removal of thymidine, cells were treated with 10μM Snap-Cell Block (New England Biolabs) according to manufacturer's instructions, and returned to MEGM culture medium for 10 hours. Media was replaced with MEGM containing Snap-Cell substrates (New England Biolabs) as indicated to label young mitochondria. After 2x washing with PBS or culture medium, the cells were either immediately taken to imaging of divisions, or returned to the incubator for additional 20 hours for post-division FACS analysis and additional labels. Snap-Cell substrates (New England Biolabs) were used as indicated for individual assays at a concentration of 1.2-3μM for Snap-Cell TMR-Star, 5μM for Snap-Cell Oregon Green, 3.3μM for Snap-Cell 360, and 5μM for Snap-Cell 430. Dyes were diluted in full media containing 0.5% BSA, and cells were labeled for 30min while being maintained at +37°C, 5% CO2.

For quantitation of asymmetric divisions, acquired images of a given time-point were merged to a composite image in ImageJ (http://rsbweb.nih.gov/ij/index.html). In case of paGFP, the time-series of pictures was scanned for cell divisions taking place during the recording, and the time-point of division was determined as the middle of the time that the dividing cell spent out of focus-plane. Intensity measurements were made from frames one-hour before and after division.

For cell cycle analysis, samples were collected at 0, 8, 16 and 24 hours after second thymidine and stained with 1ng/ml Hoechst 33342 (Life Technologies). Cells were analyzed and sorted using BD FACS Aria II SORP (Whitehead Institute) or BD FACS Aria II (University of Helsinki) cell sorters.

Analysis of mammary stem cell activity

Mammosphere culture was performed as previously described (*4*), using Corning low-adherence 24-well or 96-well plates. Cells were plated at a density of 500-1,000 cells per well in full MEGM containing 1% methylcellulose (Sigma-Aldrich). Mammosphere formation was quantified 7-12 days after plating.

Transient transfection

Cells were transfected with Lipofectamine 2000 reagent (Invitrogen) according to manufacturer's instructions. Transfection conditions were maintained for 6 hours, cells were washed twice with PBS and returned to full culture medium. Transgene expressing cells were selected by a fluorescent marker or, in case of pSNAPf-Cox8A (New England Biolabs), cells were selected with 300μg/ml geneticin for 4 days.

MitoTracker and LysoTracker labeling

For labeling of mitochondria, cells were loaded with 150nM MitoTracker Green FM (Life Technologies) or 100-150nM MitoTracker Deep Red FM (Life Technologies) for 15-20min followed by 2x washes with PBS and one wash in full medium prior to imaging or FACS analysis. For live imaging of lysosomes, cells were loaded with LysoTracker Green DND-26 (Life Technologies), diluted in full cell culture medium to a concentration of 600nM, and imaged immediately.

Inhibition of mitochondrial fission and quality control

SLCs were transfected with 50nM siRNAs targeting the human Parkin (PARK2) (J-003603-08, Dharmacon) or with non-targeting control siRNA (D-001810-01-05, Dharmacon), with Dharmafect transfection reagent according to manufacturer's instructions. Alternatively, cells were treated with 10µM mDivi-1 (Tocris) (1,000x stock in DMSO), or with DMSO (Sigma-Aldrich) as a control.

Induction of mitochondrial fission

Cells were transfected with pEYFP-C1-Drp1 (*5*) or pEYFP-C1 control plasmid as described above at indicated timepoints.

Mitochondrial membrane potential

Mitochondrial membrane potential was analyzed using the reporter dyes JC-1 as described previously (*6*), or 20nM TMRM (Invitrogen). hMECs were synchronized with a double thymidine block, and labeled with 3.3µM Snap-Cell 360 (New England Biolabs). Following washes with PBS, cells were labeled as described below and analyzed on a BD FACS Aria cell sorter immediately (1h), or replated for analysis and sorting at 30h. Cells were loaded with 20nM TMRM (Invitrogen) and 100nM MitoTracker Deep Red FM (Life Technolgies) for 15min at +37°C and washed twice with PBS, before being resuspended in full medium for analysis and sorting.

Uncoupler treatment

For imaging of hMECs treated with uncoupler, Snap-tag labeling was performed as described above. At indicated timepoints, cells were treated either with 10µM CCCP for 1h, or with 0.1-1µM CCCP for 9h (50mM stock in DMSO, Thermo Scientific). Control cells were treated with DMSO (Sigma-Aldrich). Immediately after the young label, nuclei were labeled with Hoechst 33342 (0.5µg/ml, Life Technologies). Alternatively, cells were loaded with 20nM TMRM (Invitrogen) for 30min at +37°C, followed by two washes with PBS, and imaged immediately.

For FACS analysis of the effect of CCCP on mitochondrial membrane potential, cells were cultured with CCCP (Thermo Scientific) at final concentrations of 0.1-3µM. Incubation in CCCP containing media for 17 hours was followed by PBS washes and

trypsination. Cells were labeled with 20nM TMRM (Invitrogen) for 30min at +37°C, followed by two washes with PBS, and analyzed with a BD FACS Aria cell sorter.

The effect of CCCP on cell proliferation was assessed using cells maintained in media containing 0.1-10μM CCCP (Thermo Scientific) as indicated.

For analysis of the effect of mild uncoupler treatment on asymmetric apportioning of mitochondria, cells were synchronized and Snap-tag labeled according to the protocol for asymmetry analysis described above. Following labeling of young mitochondria, cells were returned to full culture media containing 0.1-1μM CCCP (Thermo Scientific), or DMSO (Sigma-Aldrich), incubated for 17h, and collected for FACS analysis.

Analysis of mitophagy

Cells maintained in CnT-27 media were incubated with 2mM thymidine for 19 hours, trypsinized, and labeled with 5μM Snap-Cell Oregon Green (New England Biolabs) at +37°C for 30min. Following two washes with PBS, cells were plated in full culture medium on glass bottom dishes (MatTek P35G-1.5-10-C) at a density of 70,000 cells per dish, and incubated for 10 hours. Cells were returned to thymidine containing media for an additional 17 hours, followed by three washes with PBS. After release from thymidine block, cells were either fixed immediately or returned to the incubator for additional 10, 20, or 30 hours. For fixation, cells were washed with PBS before adding cold methanol and incubation at -20°C for 12min, followed by 3x washes with PBS. Following incubation in blocking buffer (10% FBS in PBS) for 1 hour at room temperature, samples were stained with primary antibody recognizing LC3b (D11 XP Rabbit mAb, Cell Signaling Technology) for 1 hour at room temperature. Subsequently, samples were washed three times with 1% BSA in PBS and incubated with Alexa Fluor A-594 coupled secondary antibody (Life Technologies) for 1 hour at room temperature. Following three washes in PBS, nuclei were stained with Hoechst 33342 (1μg/ml, Life Technologies) for 5min, and samples were washed four times with PBS prior to storage in PBS and imaging.

Analysis of mitochondrial network status

Cells were plated on glass bottom dishes (MatTek P35G-1.5-10-C) and synchronized as described above. For imaging at 0h post thymidine release, samples were labeled 1 hour prior to release while maintaining thymidine in the labeling medium. All other samples were returned to full culture media after removing thymidine and labeled at indicated timepoints. Mitochondria were loaded with 150nM MitoTracker Green FM (Life Technologies) for 20min, followed by washing in PBS and nuclear staining with Hoechst 33342 (1μg/ml, Life Technologies). Cells were then washed twice with PBS, followed by one wash with culture medium, and imaged immediately.

Confocal stacks were subjected to deconvolution using AutoQuant X3 software (Media Cybernetics), followed by three-dimensional image reconstruction with Imaris

x64 7.7.1 software (Bitplane). Modeling and quantification of the mitochondrial network was performed using Imaris FilamentTracer module (Bitplane).

Inhibition and analysis of actin dynamics

Cells were synchronized and Snap-tag labeled as described above, and actin dynamics were disrupted by treatment with Latrunculin B (Sigma-Aldrich, 2.5mM stock in DMSO) or DMSO as a control at indicated timepoints. Cells were stained for F-actin using Alexa Fluor 594 Phalloidin (Life Technologies) according to manufacturer's instructions.

Subcellular fractionation

Prior to lysis of hMECs for subcellular fractionation, protein synthesis was blocked for 30min with 60µg/ml Cycloheximide (Merck Millipore). $25x10^6$ cells were collected and lysed using a Dounce homogenizer (Sigma-Aldrich). Subcellular fractions were separated with FOCUS SubCell kit (G Biosciences) according to manufacturer's instructions.

Western blotting

Cells were collected for lysis after FACS sorting or directly from culture dishes. Lysates of subcellular fractions as well as whole cell lysates were prepared using RIPA buffer. Protein concentrations were measured using Pierce BCA Protein Assay Kit (Thermo Scientific). Western blotting was performed with Bolt Mini Gel Tank device (Life Technologies) according to manufacturer's instructions. Membranes were incubated with antibodies recognizing Snap-tag (New England Biolabs), COXIV (abcam), or Parkin (EPR5024(N), abcam) o/n at 4°C, followed by incubation with HRP-conjugated secondary antibody (Sigma-Aldrich). β-actin (Cell Signaling Technology) was used as loading control for Parkin detection. Supersignal west femto (Pierce) luminescent reagent was used for detection.

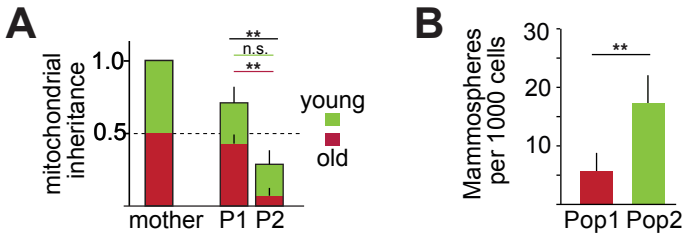

Supplementary Figure S1.
Human mammary epithelial cell line FL1 apportions old mitochondria in a similar asymmetric fashion as the FL2 cell line.
Results from live cell microscopy (A), and from mammosphere formation assay (B) with $CD44^{hi}CD24^{lo}ESA^{-}$ FL1 stem-like cells isolated from adult female breast tissue and expressing human Telomerase (3) recapitulate the findings obtained with the FL2 cell line in Figures 2C and 3D. Cell lines were separately isolated and generated (n=3, **p<0.01, t-test).

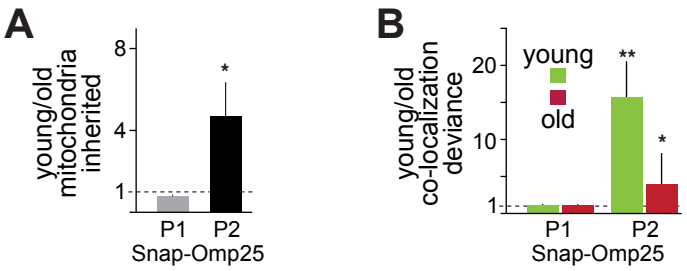

Supplementary Figure S2.
Age-selective segregation and localization of mitochondria.
(**A**) Ratio of young versus old mitochondrial label inherited by the two daughter cells. Compare to Figure 2B (n=5). (**B**) Localization of the old and young labels in the daughter cells. Ratio of total label amount and the amount that is co-localizing with the other label is presented separately for both young and old labels. In the P2 cells, particularly the young label (green) is found in regions that do not contain old label. Compare to Figure 2B (n=5). (*p<0.05, **p<0.01, t-test).

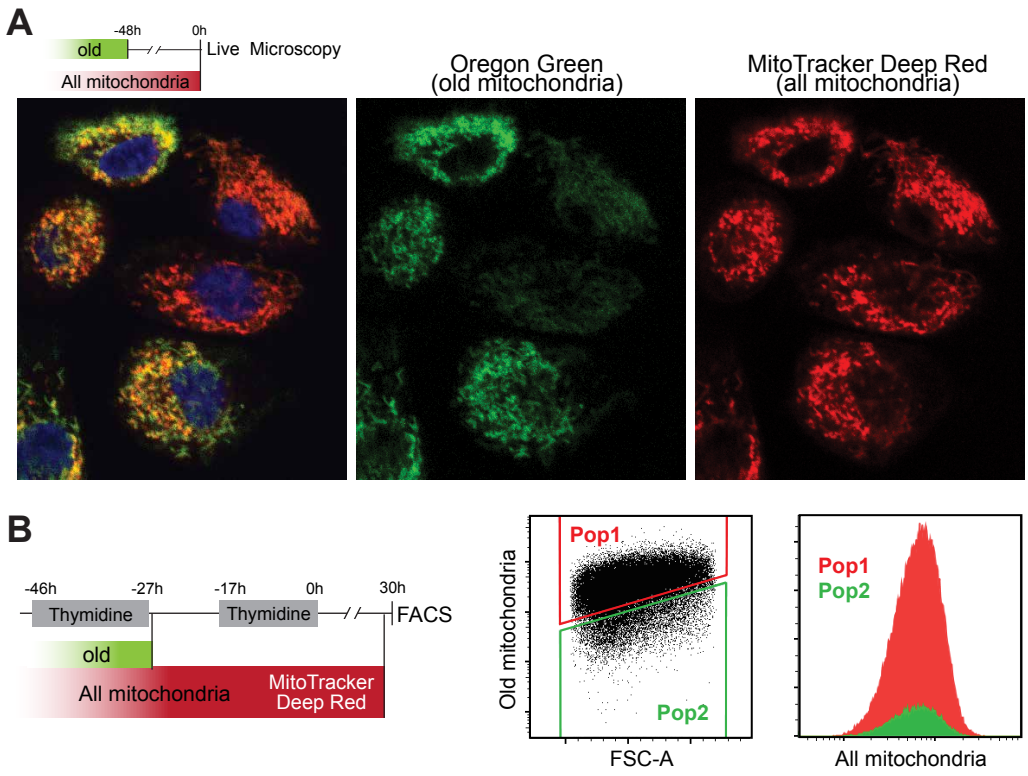

Supplementary Figure S3.
Daughter cells that receive different quantities of old mitochondria in an asymmetric cell division inherit similar amounts of total mitochondria.
(A) Live microscopy of cells 48 hours after Snap-labelling. Cells that have inherited different levels of old mitochondrial Snap-label (green) demonstrate similar labelling with MitoTracker Deep Red (red), indicating similar total mitochondria contents. Live cell imaging, 63x, 2µm Z-section. **(B)** FACS analysis of age-specific and total inheritance of mitochondria. Pop1 and Pop2 cells receive equal total amounts of mitochondria during cell divisions that apportion old mitochondria asymmetrically. Cells were analyzed by FACS for asymmetric apportioning of aged mitochondria in relation to cell size (FSC-A), and populations Pop1 and Pop2 were analyzed for the total inherited mitochondria contents with MitoTracker Deep Red.

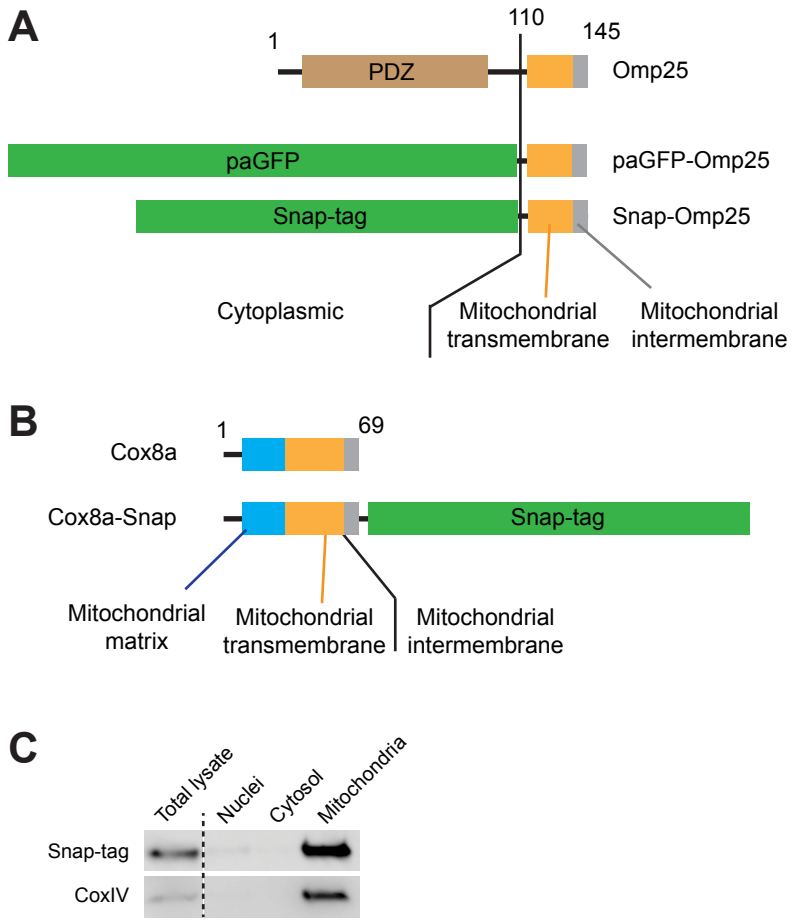

Supplementary Figure S4.
Constructs used to age-selectively label mitochondria.
(A) Targeting of the mitochondrial outer membrane. Mitochondrial outer membrane protein 25 (Omp25) is localized to the mitochondria by its C-terminal transmembrane region (118-138 aa). A C-terminal fragment (110-145 aa) that spans the transmembrane domain and the mitochondrial intermembrane domain of unknown function (139-145 aa) does not have effects on mitochondrial localization, morphology, or dynamics (7) was fused with paGFP or Snap-tag. **(B)** The mitochondrial inner membrane was targeted with the Cox8a-Snap fusion protein resulting in localization of the Snap-tag to the mitochondrial intermembrane space. **(C)** Subcellular fractionation of Snap-Omp25 expressing cells demonstrating that mitochondrially targeted Snap-tags are specifically localized to mitochondria. Fractions were probed with antibodies recognizing the Snap-tag or mitochondrial protein CoxIV.

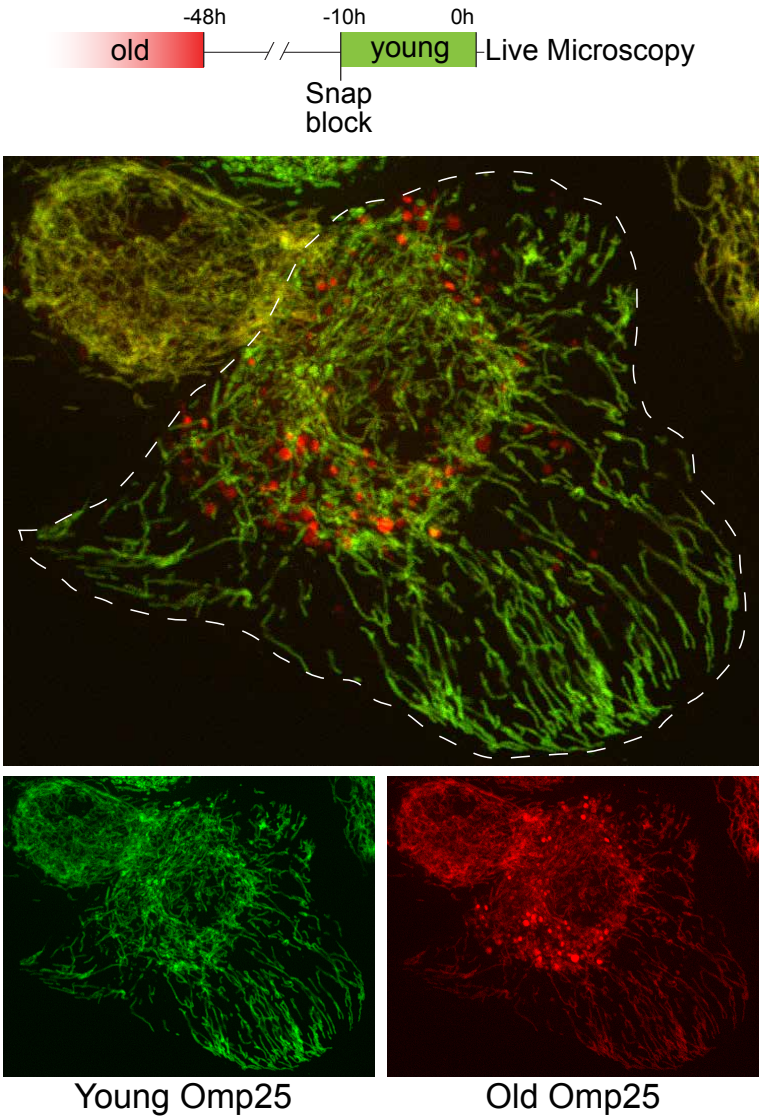

Supplementary Figure S5.
Old mitochondrial proteins are localized perinuclearly
Confocal live microscopy of a cell immediately after labelling reactions (and before division). Old (red) Snap-Omp25 is enriched in the perinuclear space, and marks both the perinuclear mitochondrial network, and in some cells, distinct puncta. Young (green) Snap-Omp25 is evenly distributed throughout the mitochondrial network. Dashed line marks a single cell. Original magnification 63x.

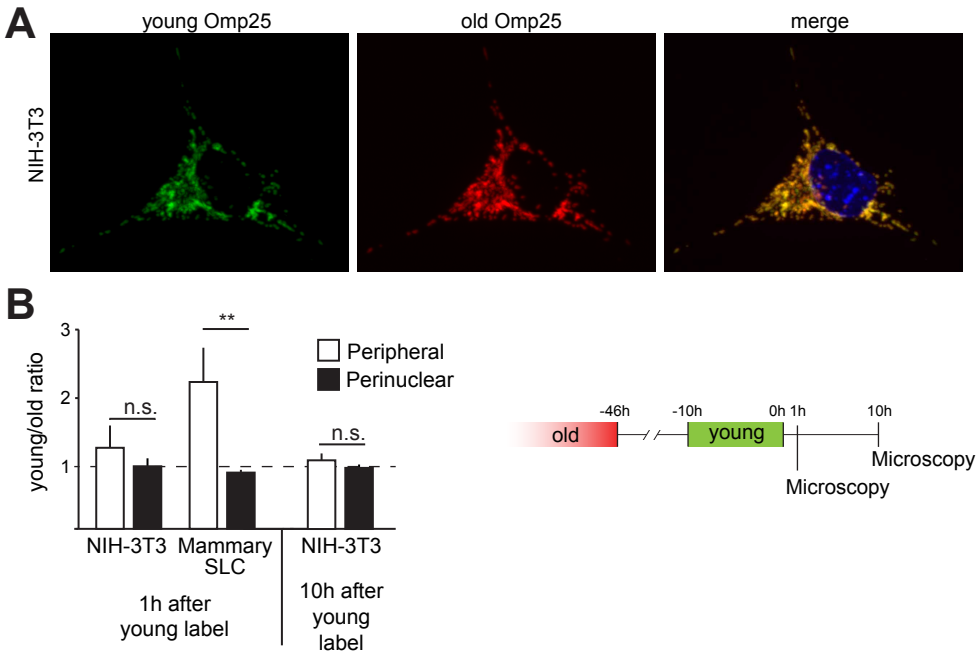

Supplementary Figure S6.
Age-specific perinuclear localization of mitochondrial proteins does not occur in cells without stem-like properties

(**A-B**) Live cell microscopy of NIH-3T3 fibroblasts and mammary SLCs expressing Snap-Omp25 and labeled according to the schematic. (**A**) Representative confocal images from NIH-3T3 cells at the first microscopy timepoint (1 hour after green label) demonstrating similar localization of the two age-classes of Snap-Omp25. Original magnification 63x. (**B**) Localization of old (red) and young (green) mitochondria (Snap-Omp25) at indicated timepoints after labeling in an undivided cell. Compare the 10-hour timepoint of NIH-3T3 to that of SLCs in Fig. 2E. n=6 (*p<0.05, **p<0.01, t-test).

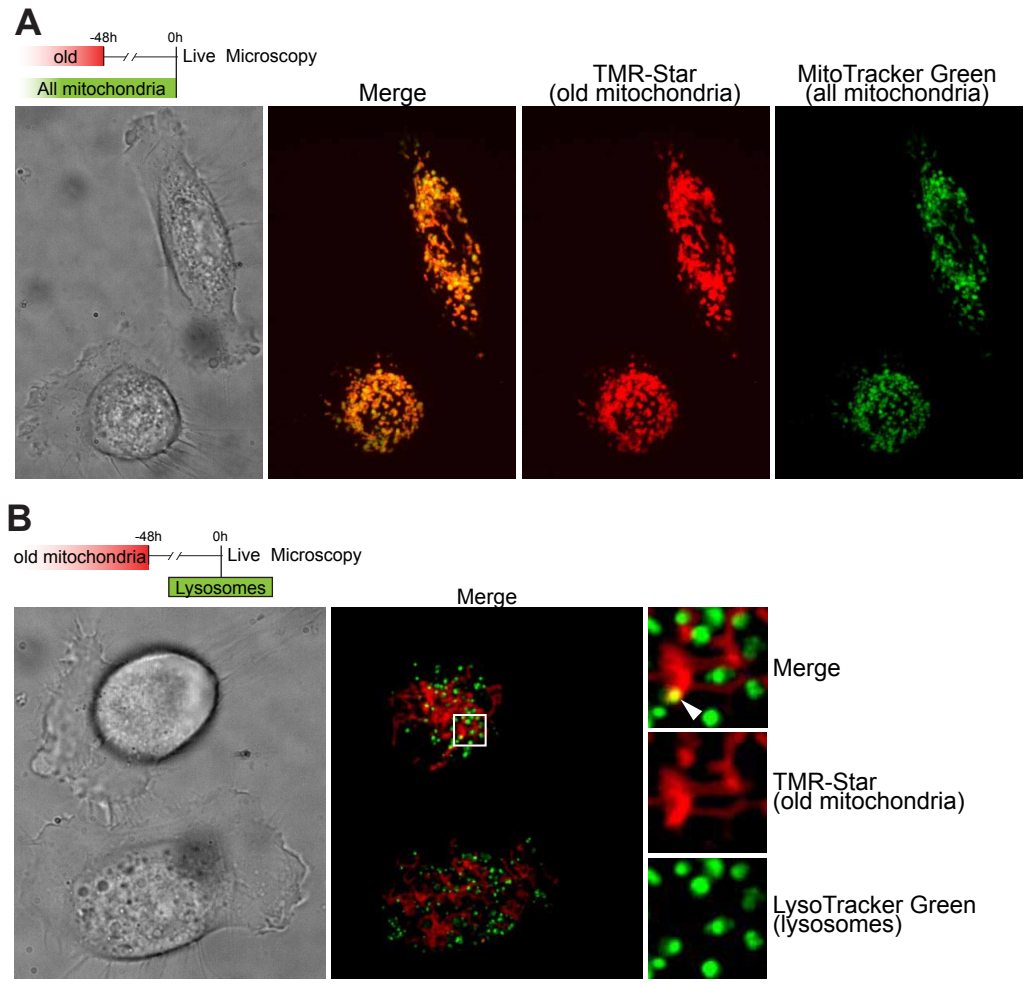

Supplementary Figure S7.
Mitochondria retain the Snap-label for extended periods of time.
(A) Live cell microscopy of cells 48 hours after Snap-labelling. The majority of mitochondrially targeted and Snap-labelled proteins reside in mitochondria and co-localize with MitoTracker Green. **(B)** Live microscopy of cells 48 hours after Snap-labelling and immediately after lysosomal labelling. A small fraction of old Snap-label is in punctate structures that co-localize with LysoTracker Green (arrowhead), indicating degradation of some old mitochondrial proteins via the autophagosomal-lysosomal pathway. 63x Live cell imaging of the whole cell height (A) or a 1 µm Z-section (B).

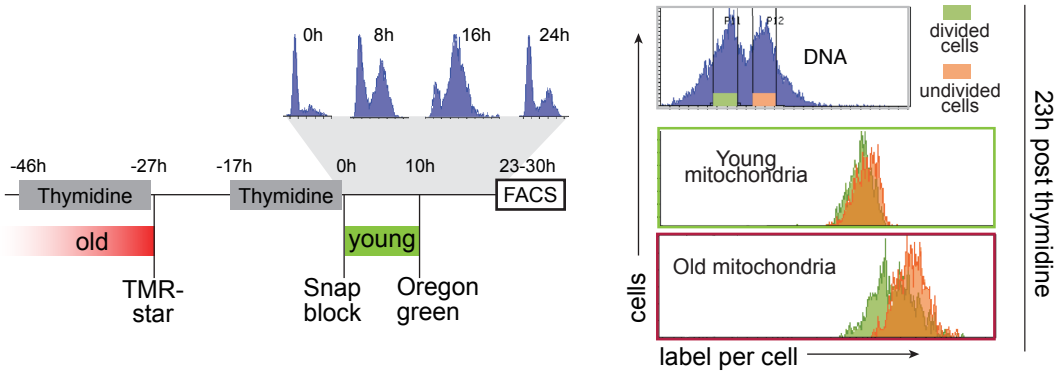

Supplementary Figure S8.
Age-selective segregation of mitochondrial tags in cells undergoing synchronized cell division.
Schematic of experiments with synchronized cells, and FACS analyses comparing content of old and young mitochondria (Snap-Omp25) in cells that have divided to cells that have not yet undergone division. Cells that divided have half the DNA content (top histogram, light green) of the undivided cells (light orange), and contain two populations with either fewer, or almost as many old mitochondria as the undivided cells. In contrast, all cells have similar amounts of young mitochondrial label after division.

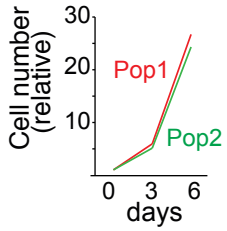

Supplementary Figure S9.
Sorted Pop1 and Pop2 cells proliferate with similar rates.
Proliferation of FACS-sorted populations Pop1 and Pop2 was followed for 6 days in 2D-culture that does not favor stem-like cells.

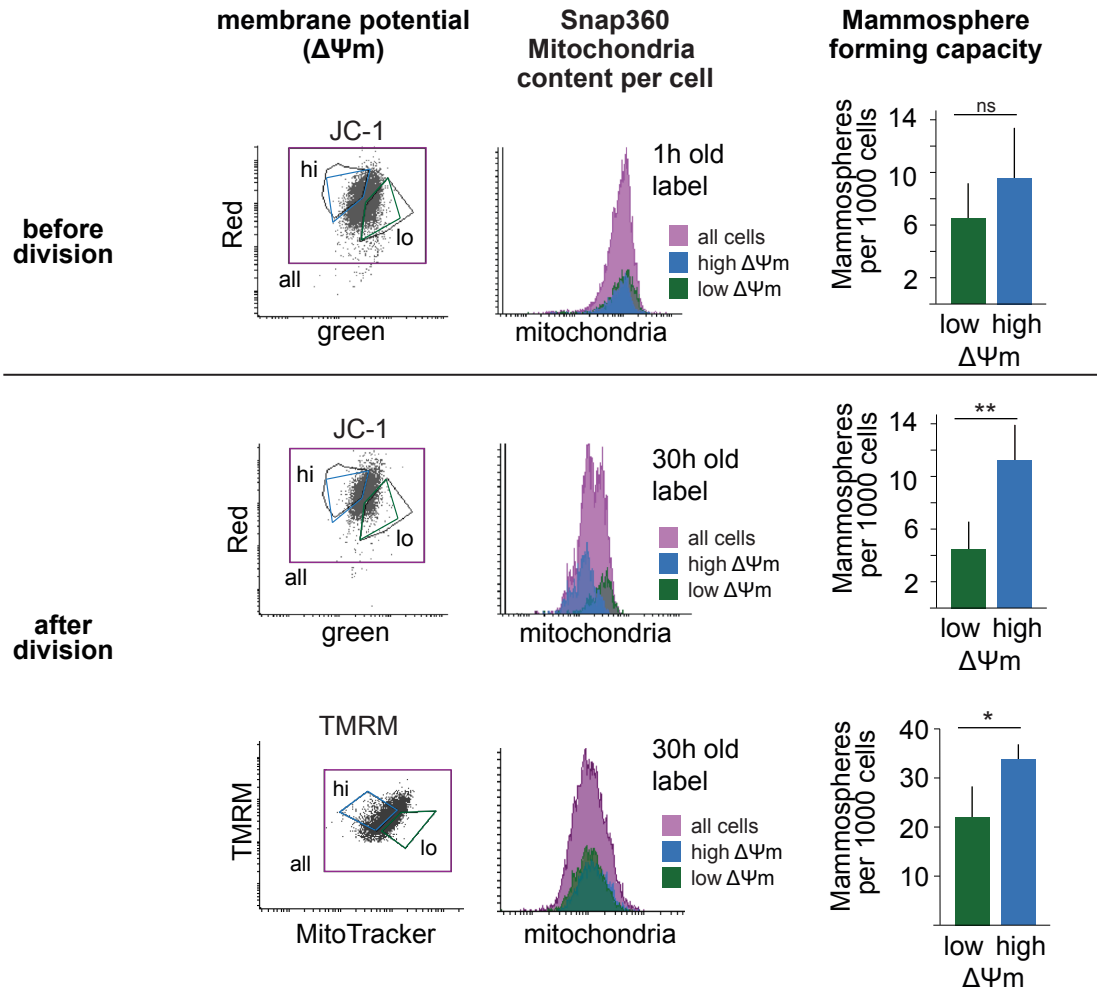

Supplementary Figure S10.
Mitochondrial membrane potential does not correlate with the age of inherited mitochondria based on Nernstian markers.
FACS Analysis of mitochondrial membrane potential in cells inheriting different amounts of old mitochondria. Two mitochondrial membrane potential indicators, tetrachloro-tetraethylbenzimidazolylcarbocyanine iodide (JC-1) and tetramethylrhodamine methyl ester (TMRM), were used and old mitochondria were labelled with Snap360. Snap360 labelling was performed immediately after release from the cell cycle block, allowing us to observe the apportioning of mitochondria that were at least 20 hours old upon cell division. All synchronized cells had equal amounts of Snap-labelled mitochondria immediately after Snap360 labelling (before division), and the labelled mitochondria were asymmetrically apportioned upon division to yield two populations with approximately a 2-fold difference in old mitochondria content (after division). With JC-1, cells with high membrane potential after division (hi, blue) inherited fewer old mitochondria than cells with low membrane potential (green). However, with TMRM, there was no difference in the quantity of old mitochondria between high and low ΔΨm cells. The lower red fluorescence of JC-1 observed in cells containing old mitochondria may therefore reflect ΔΨm-independent characteristics of JC-1 (*8,9*). Cells with high mitochondrial membrane potential have higher mammosphere forming capacity according to both dyes. (n=3, *p<0.05, **p<0.01).

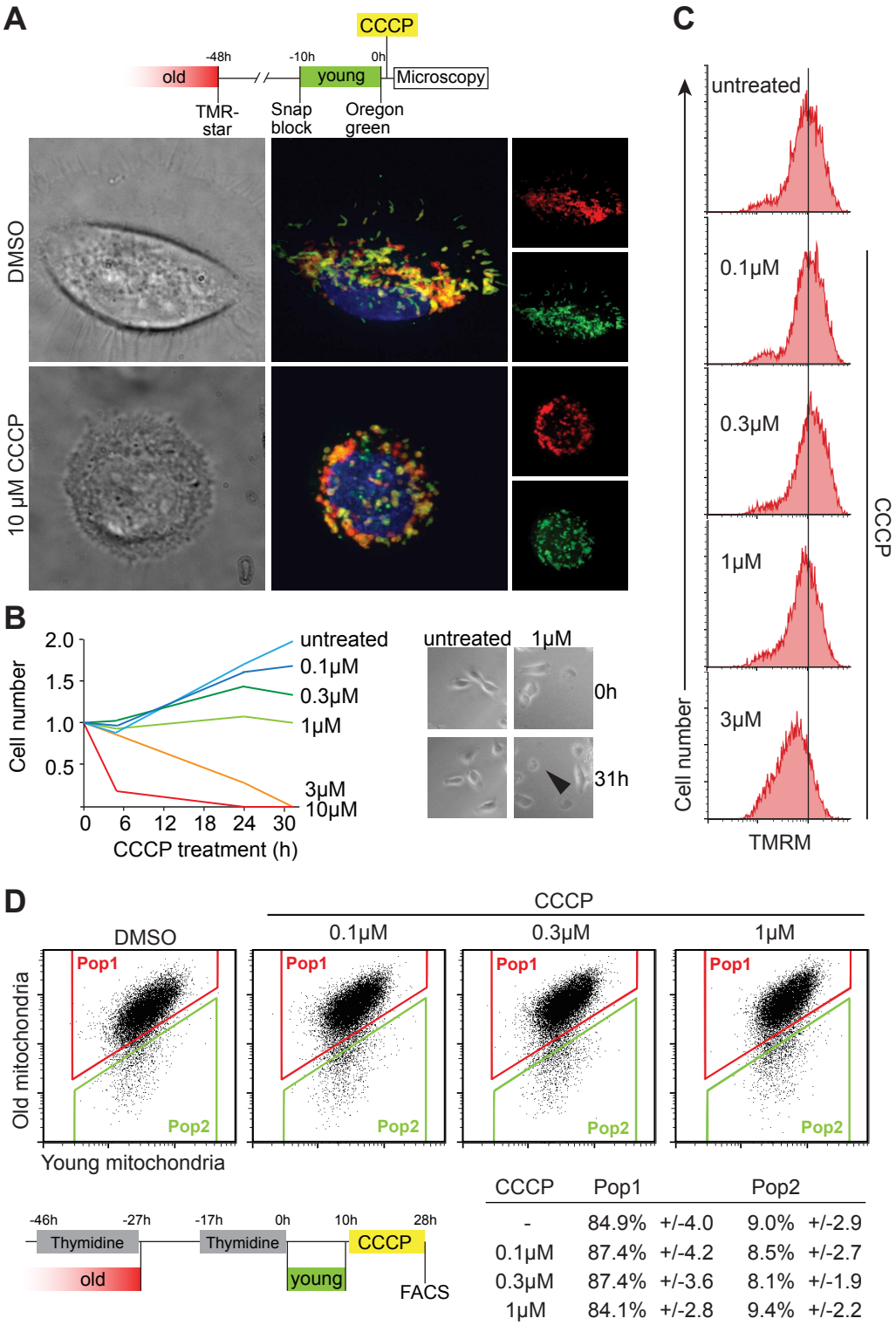

CCCP	Pop1		Pop2	
-	84.9%	+/-4.0	9.0%	+/-2.9
0.1µM	87.4%	+/-4.2	8.5%	+/-2.7
0.3µM	87.4%	+/-3.6	8.1%	+/-1.9
1µM	84.1%	+/-2.8	9.4%	+/-2.2

Supplementary Figure S11. Katajisto et al

Supplementary Figure S11.

Uncoupler-induced alterations of mitochondrial membrane potential do not alter the capacity of SLCs to age-selectively segregate mitochondria.

(A) Uncoupler treatment causes fragmentation of the mitochondrial network. Cells treated with 10 μM of the mitochondrial uncoupler CCCP for 1 hour showed fragmentation of young and old mitochondria, whereas DMSO treated cells had mitochondria with normal morphology. Live cell imaging with nuclei stained with Hoechst, 63x, 4 μm Z-section. **(B)** Analysis of cell proliferation and cell death with indicated concentrations of CCCP. CCCP impairs proliferation and induces cell death (micrograph, arrowhead) in hMECs at concentrations ≥ 1μM. **(C)** FACS analysis of mitochondrial membrane potential following CCCP treatment. TMRM staining intensity indicates a compensatory increase in mitochondrial membrane potential in cells treated with 0.1-0.3 μM CCCP. The reduction in TMRM fluorescence and increase in the frequency of TMRM-negative cells indicate that compensatory mechanisms fail to maintain membrane potential at ≥ 1μM CCCP. **(D)** Asymmetric and age-selective apportioning of mitochondria is maintained during uncoupler treatment. Treatments with CCCP at concentrations that allow analysis of cell divisions (based on A-C) do not significantly alter asymmetric apportioning of aged mitochondria (n=3-5 per treatment).

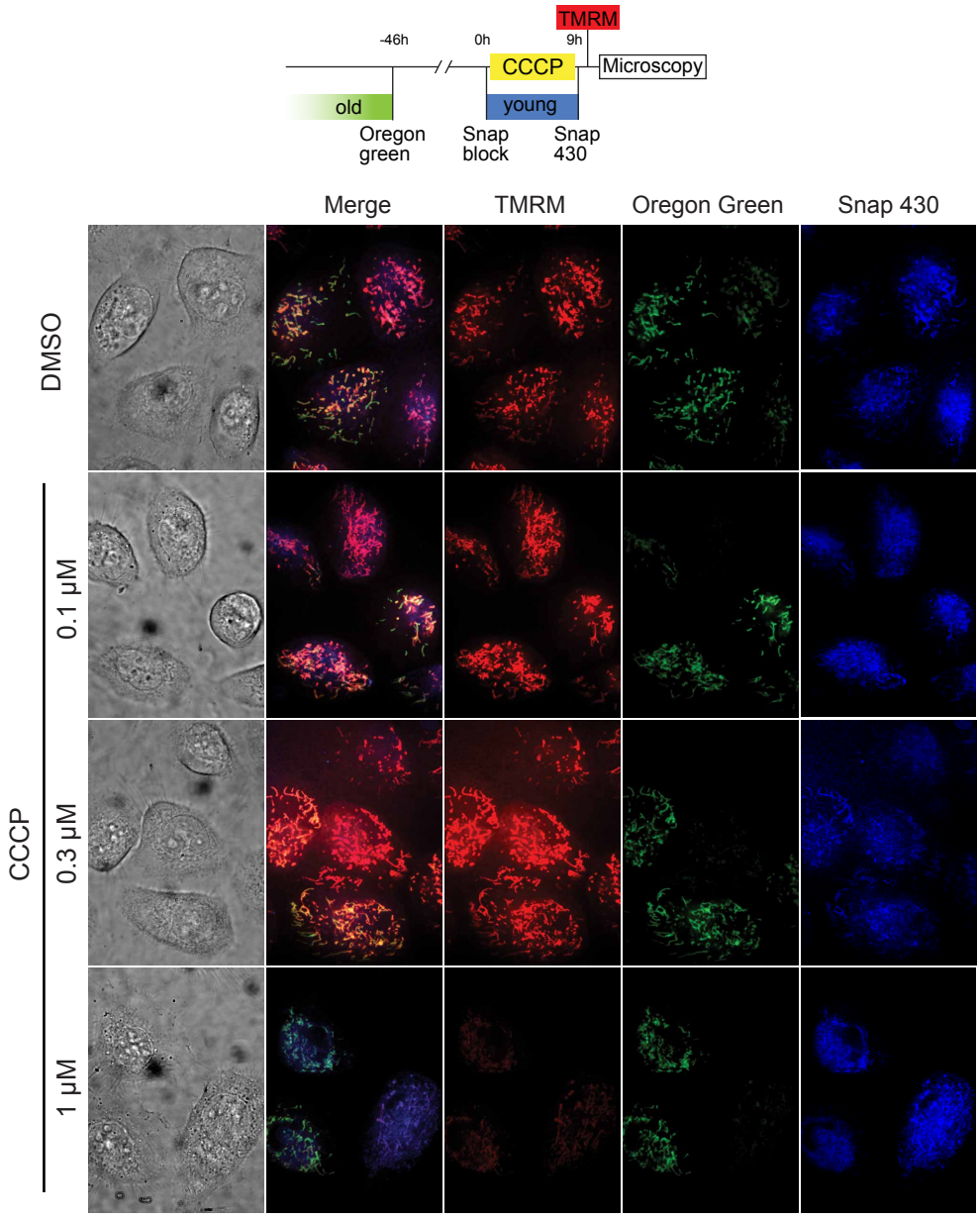

Supplementary Figure S12.
Uncoupler treatment alters mitochondrial membrane potential regardless of the age of inherited mitochondria.
Cells that have inherited different levels of old mitochondria (green) based on Snap-labelling, respond similarly to CCCP treatment by modulating their mitochondrial membrane potential. Note the slight increase in TMRM fluorescence at 0.1-0.3 µM CCCP and the reduction at 1 µM CCCP, which corroborates the data from FACS analysis in Figure S11C. Live cell imaging, 63x, 0.5 µm Z-sections.

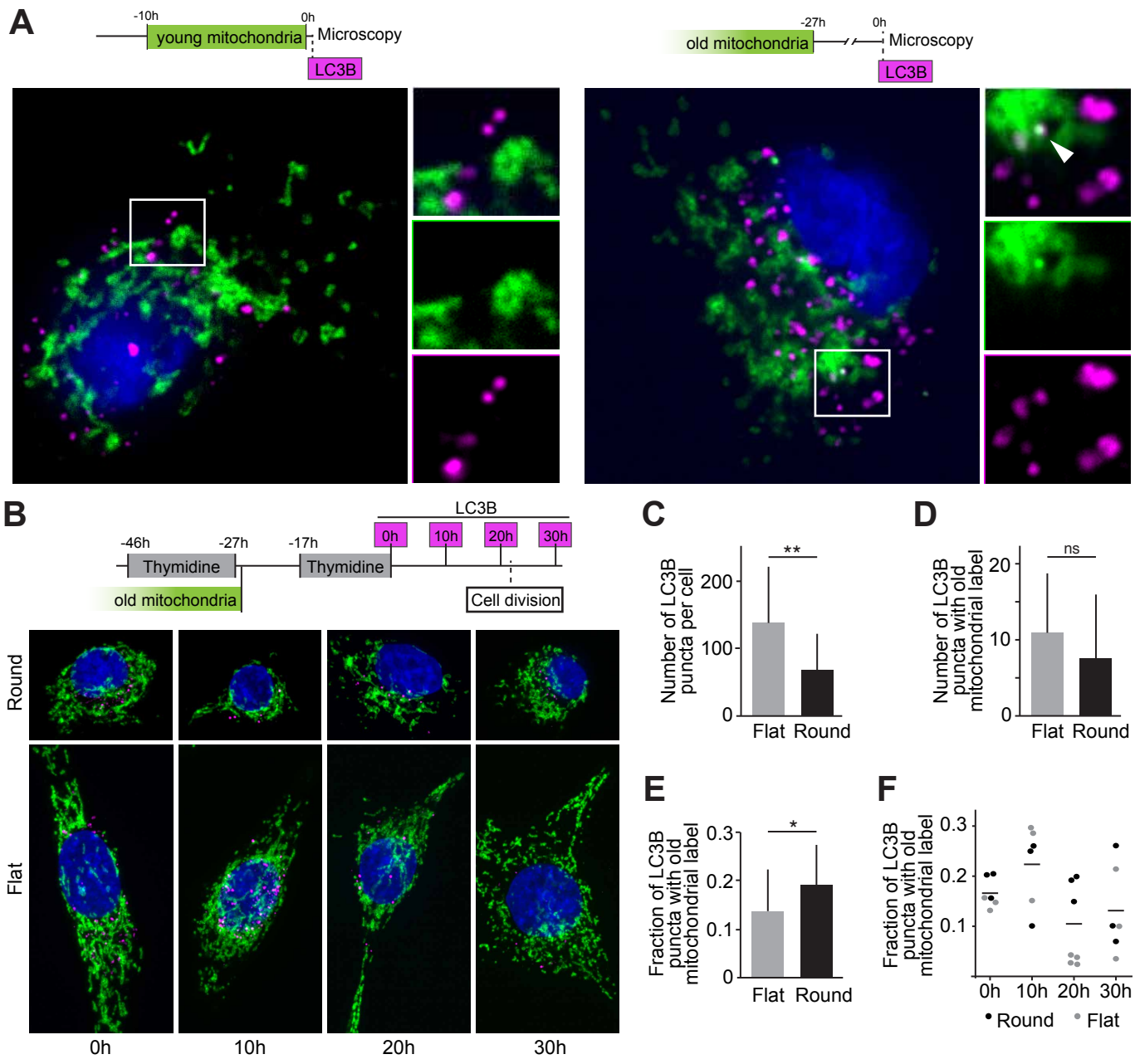

Supplementary Figure S13.
Differential mitophagy does not cause the difference in old mitochondria amounts between daughter cells.
(A) Analysis of autophagy of old and young mitochondria. Images show a single confocal plane of cells that were stained for LC3B after Snap-tag labelling of young (left panel) or old (right panel) mitochondria. A small fraction of old mitochondrial label (older than 27h) co-localized with autophagosomes (arrowhead), whereas we rarely observed an overlap of LC3B with young mitochondrial label (younger than 10 h). **(B-D)** Morphologically flat differentiated cells have a higher number of autophagosomes, but there is no significant difference in mitophagy between differentiated cells and SLCs. Cells that were Snap-tag labelled for old mitochondria were stained for LC3B at indicated time points, allowing for analysis of autophagy and mitophagy during the entire cell cycle. (B) Representative images of morphologically round and flat cells at indicated time points (1.5 µm Z-sections). (C) Average number of autophagosomes per cell, as represented by the total number of LC3B puncta per cell (n=24). (D) Average number of autophagosomes that contain old mitochondrial label (n=24). **(E,F)** Round SLCs dedicate a larger relative fraction of autophagosomes to mitophagy, but mitophagy does not change significantly during the cell cycle. Fraction of the old mitochondrial label containing autophagosomes is presented as the mean (E, n=24) and at indicated time points of the cell cycle (F, each data point represents a single cell). *p<0.05, **p<0.01, t-test.

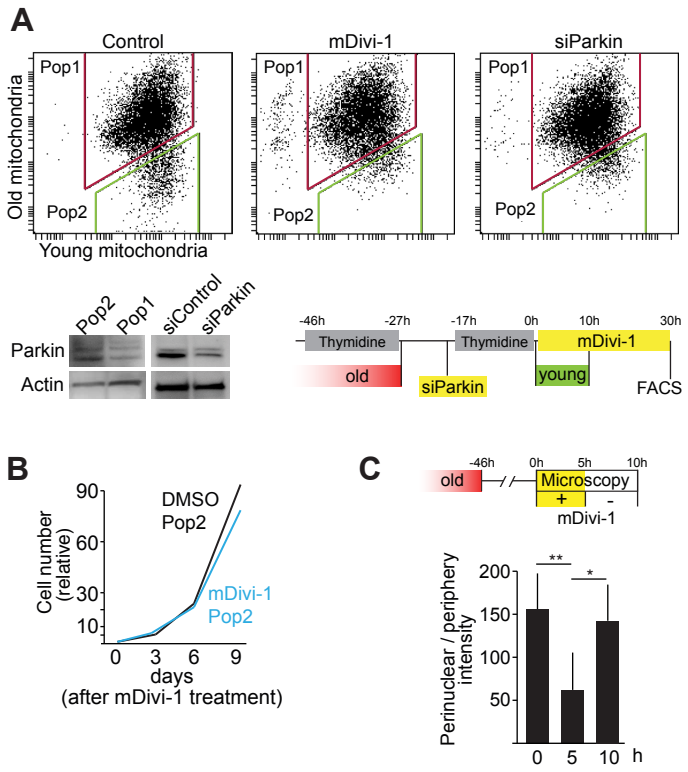

Supplementary Figure S14.
Effects of mitochondrial quality control on asymmetric apportioning of old mitochondria during cell division.
(A) FACS analyses of mitochondrial apportioning in cells with defective mitochondrial quality control induced by siRNA-mediated knock-down of Parkin (siParkin) or by pharmacological inhibition of mitochondrial fission (mDivi-1). Both treatments depleted the population of cells that inherited fewer old mitochondria (Pop2). The median ratio of old/young mitochondria in the remaining Pop2 cells was also reduced from 48 in control samples to 9 and 8 in siParkin and mDivi-1 treated samples, respectively. The loss of asymmetry in SLC divisions with mDivi-1 was likely due to partial inhibition of mitochondrial fission, because complete loss of Drp1 is reported to result in clustered mitochondria that are inherited unequally by the daughter cells (*10*). **(B)** Proliferation of Pop2 in 2D-culture was unaffected by treatment with 10 μM mDivi-1. Moreover, cytokinesis is unaffected by Drp1 loss (10), further suggesting that the effects on mammosphere formation (Fig. 4B) could not be attributed to the cytotoxic effects of mDivi-1. **(C)** Localization of old mitochondria following treatment with mDivi-1. Perinuclear and peripheral intensities of old mitochondrial label at 0, 5, and 10 hours is presented, with mDivi-1 treatment during 0-5 hours. The perinuclear localization of old mitochondrial label was restored by removal of mDivi-1. (n=3, *p<0.05, **p<0.01, t-test).

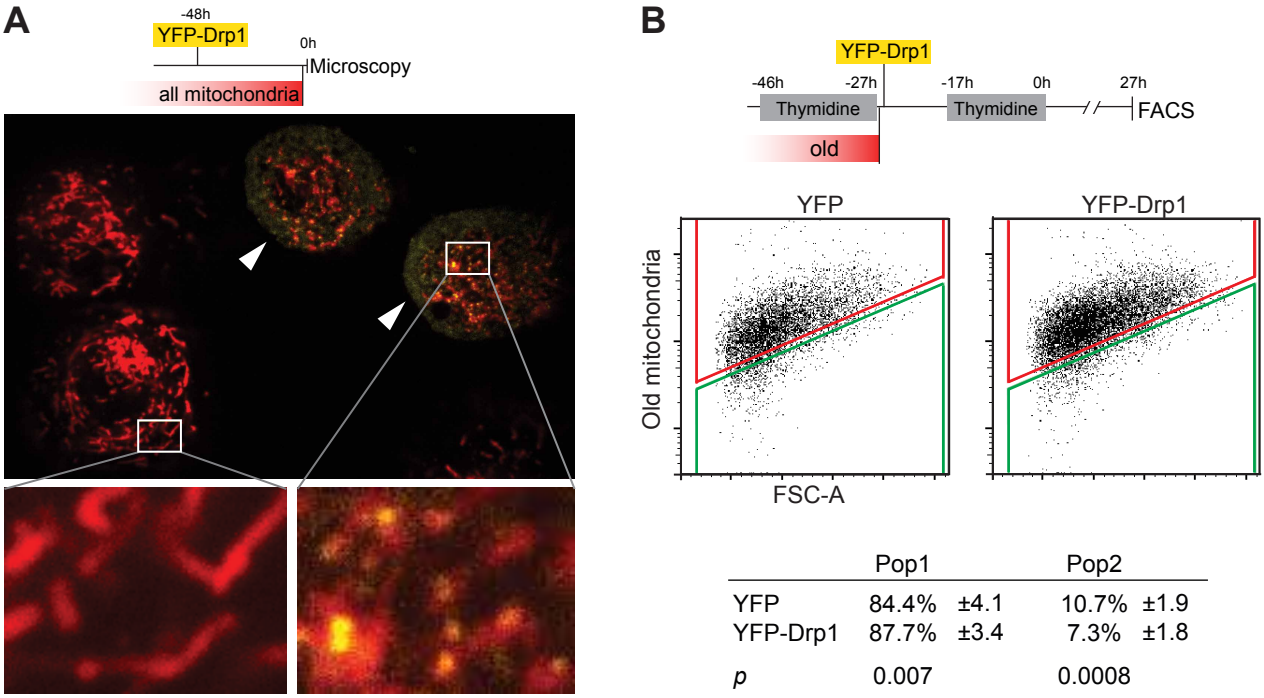

	Pop1		Pop2	
YFP	84.4%	±4.1	10.7%	±1.9
YFP-Drp1	87.7%	±3.4	7.3%	±1.8
p	0.007		0.0008	

Supplementary Figure S15.
Fragmentation of mitochondria by overexpression of Drp1 inhibits asymmetric segregation of old mitochondria.
(A) Drp1 overexpression induces fragmentation of mitochondria in hMECs. Cells transfected with YFP-Drp1 (yellow, arrowheads) and non-transfected cells are shown. The entire mitochondrial network was labelled red with MitoTracker Deep Red FM. YFP-Drp1 forms punctate structures localizing to mitochondria, and mitochondria are more fragmented in YFP-Drp1 positive cells (63x, single confocal plane). **(B)** Drp1 overexpression decreased asymmetric apportioning of aged mitochondria. Cells expressing similar levels of YFP-Drp1, or YFP were selected for FACS analysis of asymmetric inheritance of Snap-labelled aged mitochondria. Drp1 expressing cells showed a significant reduction in cells that did not inherit old mitochondria (Pop2) (n=8, t-test).

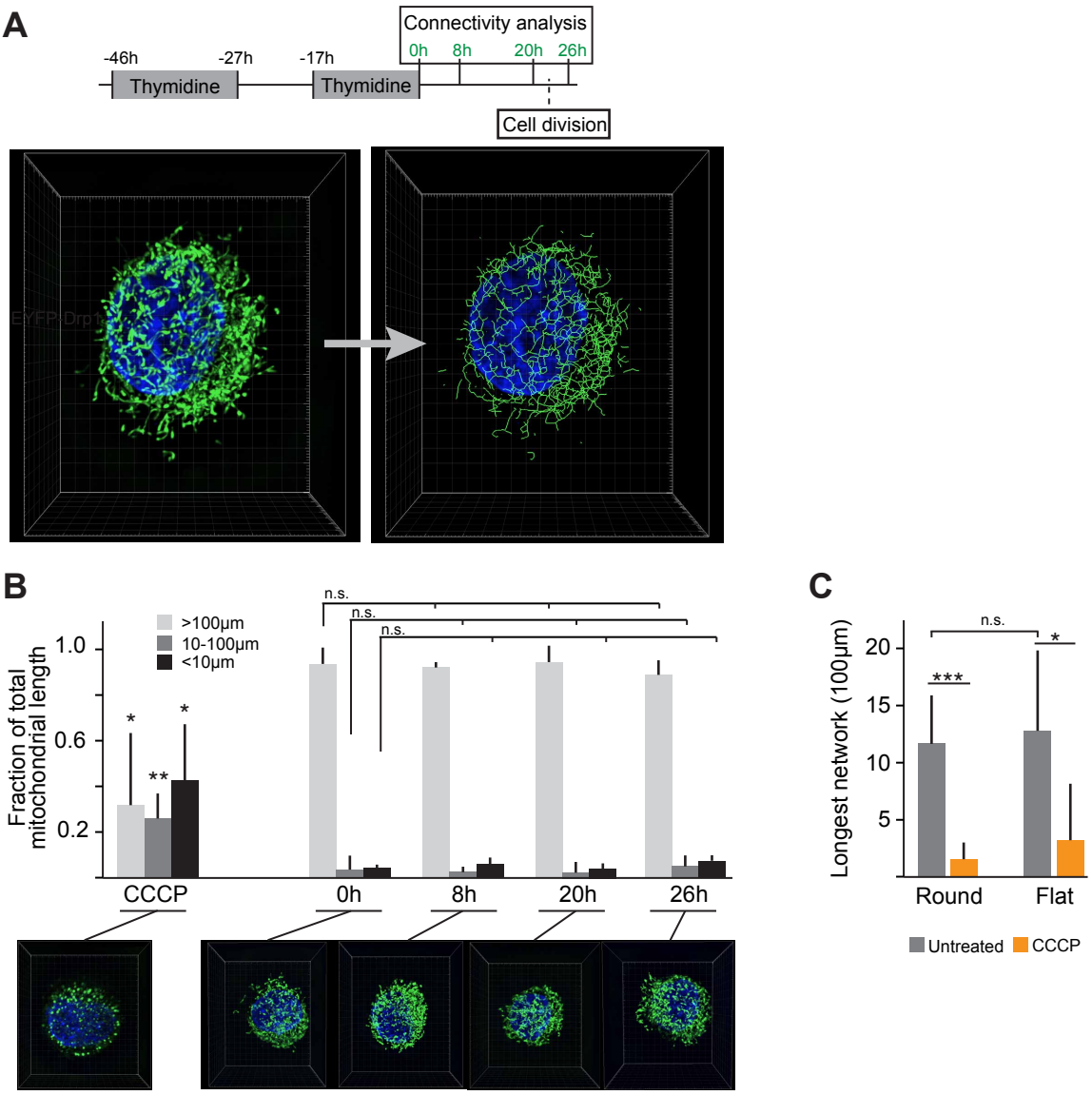

Supplementary Figure S16.
Mitochondrial networks of SLCs and differentiated cells have similar overall topology and connectivity.
(A) Analysis of the mitochondrial network connectivity. Three-dimensional mitochondrial networks were reconstructed from live cells labelled with MitoTracker Green (left) and converted to a network projection (right). Absolute length and size distribution of individual components of the mitochondrial network were used to assess the network status of individual cells. **(B)** Morphologically round SLCs show no significant changes in mitochondrial connectivity during the cell cycle. Network status was analyzed at indicated time points after thymidine release. Network components were binned according to their length (<10 µm, 10-100 µm, >100 µm), and CCCP-induced fragmentation was used as a control. Connectivity status does not change significantly during the cell cycle. In particular, the time points around the cell division demonstrate that changes in mitochondrial network connectivity do not underlie age-specific localization and segregation of mitochondrial proteins (n=5-7 cells per time point). **(C)** Mitochondria of differentiated cells and stem-like cells have similar network connectivity. In the majority of cells, a single interconnected network contained most of the mitochondria, and its length was analyzed as a measure of network status based on pooled analysis of different time points during the cell cycle (n=25 for round cells and n=12 for flat cells). CCCP-treated controls were used as controls (n=5 round cells and n=4 flat cells). (*p<0.05, **p<0.01, ***p<0.001, n.s. not significant, t-test).

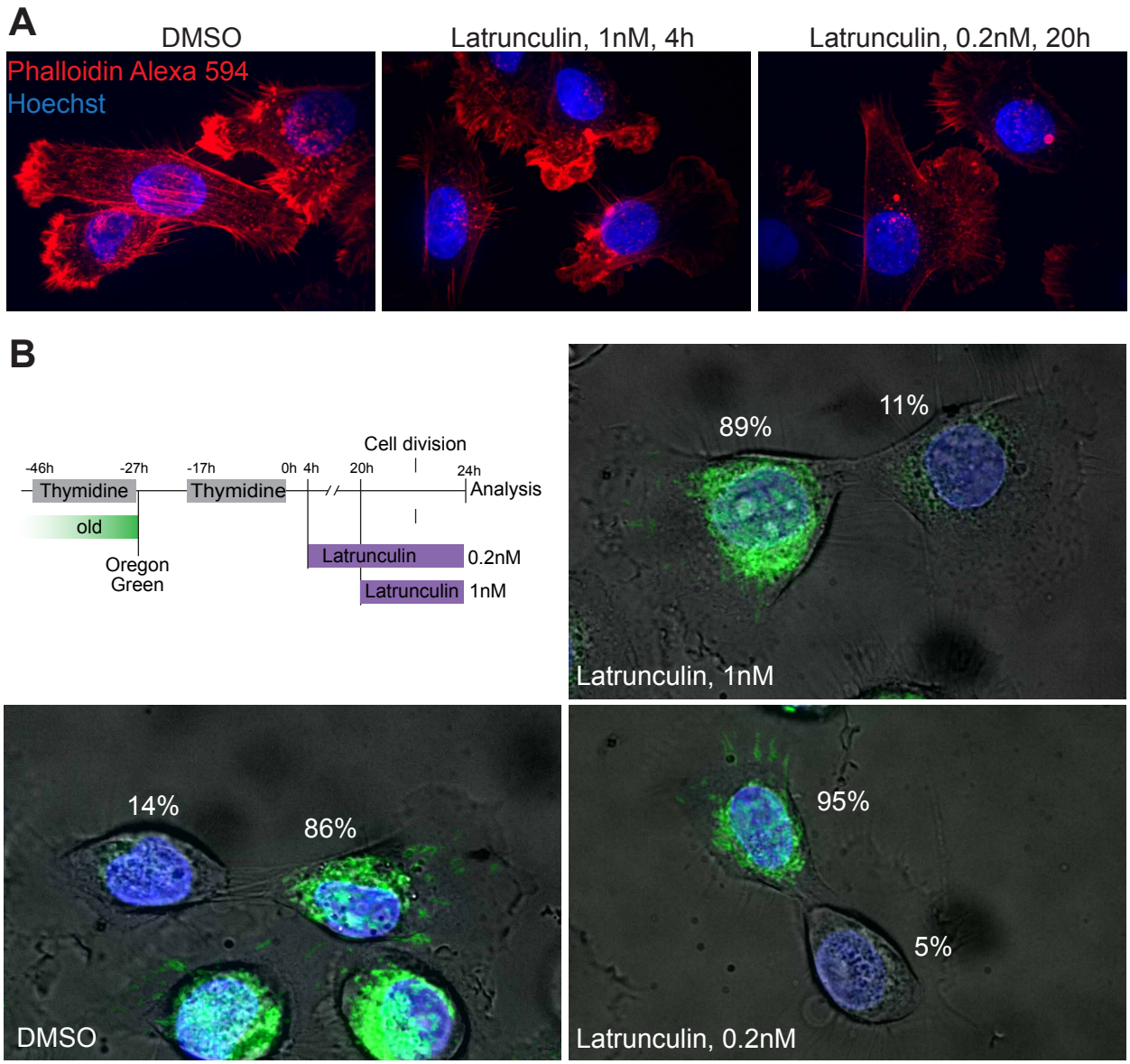

Supplementary Figure 17
Asymmetric segregation of old mitochondrial proteins is not sensitive to alterations in actin dynamics.
(A) Actin dynamics were inhibited by 4 or 20 hour long treatments with 1 nM and 0.2 nM Latrunculin B, respectively. Both treatments had notable effects on actin cytoskeleton as analyzed by phalloidin staining. **(B)** Old mitochondria (Snap-Omp25, green) can be apportioned asymmetrically between the daughter cells of SLCs despite altered actin dynamics. Percent values indicate the per cell portion of total old mitochondria in the two daughters.

Table S1.

Organelles targeted with fusion proteins containing photoactivatable GFP, and the orientation of the targeting constructs

Targeted organelle	localization marker	N- or C-term paGFP
mitochondria	OMP25	N
lysosome	Lamp-2	C
Golgi	1,4-galactosyltransferase (81 N-term aa)	N
ribosomes	Rpl10a	N
chromatin	histone 2-B	C

Supplementary movie S1

Division of a morphologically round stem-like human mammary epithelial cell expressing mitochondrial paGFP (Omp25–paGFP) (green), and stained by the endocytosed lipid-dye PKH26 (red). Note the division in the left side of the view. Capture rate: 1 frame per 3 minutes.

Supplementary movie S2

Division of morphologically flat human mammary epithelial cells expressing mitochondrial paGFP (Omp25–paGFP) (green), and stained by the endocytosed lipid-dye PKH26 (red). Note the two divisions in the middle of the view. Capture rate: 1 frame per 3 minutes.

Supplementary movie S3

Division of a morphologically round stem-like human mammary epithelial cell expressing mitochondrial Snap-tag (Omp25–Snap), and stained by TMR-Star (red) and Oregon Green (green) containing Snap-tag substrates respectively at 54 and 6 hours before division. Note the division in the top left of the view. Capture rate: 1 frame per minute.

Supplementary movie S4

Perinuclear localization of old mitochondrial label (TMR-Star staining at 46 hours before the start of microscopy) is dissipated by inhibition of mitochondrial fission with mDivi-1 treatment at the start of microscopy. Capture rate: 1 frame per minute.

Supplementary movie S5

Three-dimensional reconstruction of confocal stacks of mitochondria (MitoTracker Green FM), and model of the mitochondrial network. Nucleus is stained with Hoechst 33342.

Supplementary references

1. Y. Sancak *et al.*, The Rag GTPases bind raptor and mediate amino acid signaling to mTORC1. *Science* **320**, 1496 (Jun 13, 2008).
2. G. H. Patterson, J. Lippincott-Schwartz, A photoactivatable GFP for selective photolabeling of proteins and cells. *Science* **297**, 1873 (Sep 13, 2002).
3. C. L. Chaffer *et al.*, Normal and neoplastic nonstem cells can spontaneously convert to a stem-like state. *Proceedings of the National Academy of Sciences of the United States of America* **108**, 7950 (May 10, 2011).
4. G. Dontu *et al.*, In vitro propagation and transcriptional profiling of human mammary stem/progenitor cells. *Genes & development* **17**, 1253 (May 15, 2003).
5. S. Frank *et al.*, The role of dynamin-related protein 1, a mediator of mitochondrial fission, in apoptosis. *Developmental cell* **1**, 515 (Oct, 2001).
6. S. T. Smiley *et al.*, Intracellular heterogeneity in mitochondrial membrane potentials revealed by a J-aggregate-forming lipophilic cation JC-1. *Proceedings of the National Academy of Sciences of the United States of America* **88**, 3671 (May 1, 1991).
7. M. N. Serasinghe, Y. Yoon, The mitochondrial outer membrane protein hFis1 regulates mitochondrial morphology and fission through self-interaction. *Experimental cell research* **314**, 3494 (Nov 15, 2008).
8. C. Chinopoulos, L. Tretter, V. Adam-Vizi, Depolarization of in situ mitochondria due to hydrogen peroxide-induced oxidative stress in nerve terminals: inhibition of alpha-ketoglutarate dehydrogenase. *Journal of neurochemistry* **73**, 220 (Jul, 1999).
9. S. W. Perry, J. P. Norman, J. Barbieri, E. B. Brown, H. A. Gelbard, Mitochondrial membrane potential probes and the proton gradient: a practical usage guide. *BioTechniques* **50**, 98 (Feb, 2011).
10. N. Ishihara *et al.*, Mitochondrial fission factor Drp1 is essential for embryonic development and synapse formation in mice. *Nature cell biology* **11**, 958 (Aug, 2009).